



# Population synthesis of $s$ -process element enhanced stars: Constraining the $^{13}\text{C}$ efficiency

A. Bonačić Marinović, R.G. Izzard, M. Lugaro and O.R. Pols

Sterrenkundig Instituut, Universiteit Utrecht, P.O. Box 80000, NL-3508 TA  
Utrecht, The Netherlands.  
e-mail: bonacic@astro.uu.nl

**Abstract.** We study  $s$ -process element abundance ratios in stars by carrying out stellar population synthesis, using a rapid synthetic stellar evolution code which includes an up-to-date treatment of AGB nucleosynthesis and evolution. In contrast to other studies, we find that a large spread in the  $^{13}\text{C}$  efficiency parameter ( $^{13}\text{C}_{\text{eff}}$ ) is not needed to explain the observed spread in the ratios of heavy  $s$ -process to light  $s$ -process elements ( $[\text{hs}/\text{ls}]$ ), but this comes naturally from the range of different initial stellar masses and their time evolution. As a result, the  $^{13}\text{C}$  efficiency needed for fitting most stars in the galactic disk is constrained to  $1 \lesssim ^{13}\text{C}_{\text{eff}} \lesssim 2$ . In the same fashion we also study the  $[\text{Pb}/\text{Ce}]$  ratios of lead stars and find out that for low metallicities  $^{13}\text{C}_{\text{eff}} \sim 0.5$ .

## 1. Introduction

$S$ -enhanced stars show high abundances of elements heavier than Fe compared to the Sun, which are produced via slow neutron capture processes ( $s$ -process elements). These  $s$ -process elements are synthesized during the thermally pulsing asymptotic giant branch (TP-AGB) phase in low and intermediate mass stars, however, there are also less evolved stars which show over-abundances of these elements, thus  $s$ -enhanced stars are classified as intrinsic and extrinsic. Intrinsic  $s$ -enhanced stars (TP-AGB or post-AGB stars) produce their own  $s$ -process elements including the radioactive element Tc, which is observed in their envelopes would have already decayed if it was not produced in situ. These stars are factories of  $s$ -process elements in the universe so understanding

them is crucial to the understanding of the chemical evolution of heavy elements in galaxies. On the other hand, extrinsic  $s$ -enhanced stars are not yet evolved enough to be in the TP-AGB phase, but have accreted mass enriched with  $s$ -process elements from an intrinsic  $s$ -enhanced companion in a binary system. Thus they show an overabundance of stable  $s$ -process elements, but no signatures of Tc. The study of these stars is useful for probing the nucleosynthesis that occurred in their WD companions when they were on the TP-AGB phase, and it also provides information about stellar interaction in wide binary systems, e.g., on the different modes of mass transfer and tidal interaction.

Detailed stellar evolution and nucleosynthesis models must be able to reproduce the abundances of both intrinsic and

extrinsic *s*-enhanced stars. Testing the absolute elemental abundances directly turns out to be difficult because they depend on the dilution of material from the inter-shell into the envelope, which in turn depends on several uncertain features such as the amount of dredge up, mass loss, mass accretion, etc. However, the *s*-process element abundance ratios are practically unaffected by these processes. They provide useful constraints on another important uncertain parameter: the total neutron flux. This is determined in the models of Gallino et al. (1998) by setting the amount of  $^{13}\text{C}$  nuclei ( $^{13}\text{C}$  efficiency, i.e.,  $^{13}\text{C}_{\text{eff}}$ ), which act as the main neutron source via the  $^{13}\text{C}(\alpha, n)^{16}\text{O}$  reaction during the interpulse periods. Gallino et al. (1998) also introduce a  $^{13}\text{C}_{\text{eff}}$  scale where the standard case (ST in their paper, i.e.,  $^{13}\text{C}_{\text{eff}} = 1$ ) corresponds to the amount of  $^{13}\text{C}$  needed for a  $1.5 M_{\odot}$  AGB star with half solar metallicity to produce the main *s*-process element abundance of the Sun. It was subsequently found that a wide spread in  $^{13}\text{C}_{\text{eff}}$  (around two orders of magnitude) is needed for the detailed models to reproduce the spread in abundance ratios from the observational data (e.g., Busso et al., 2001, Gallino et al., 2005, and references therein). However, for computing time reasons, these authors used only a limited number of initial masses for their models and only compared to the observations the abundances for a “typical” thermal pulse. By carrying out stellar population synthesis with a rapid synthetic code, we can make models for a much finer grid of initial masses and also take into account the time evolution of the abundances. We can thus produce a much larger set of synthetic data, and weight the results with the initial mass function (IMF), in order to compare to observations in a statistical sense. Thus we are able to find better constraints on the  $^{13}\text{C}$  efficiency parameter.

## 2. Population synthesis

We carry out the population synthesis with a rapid synthetic evolution code based on

that from Izzard et al. (2004), but modified to be more self-consistent with the evolutionary phases prior to the TP-AGB (Bonacic et al. in preparation). The *s*-process nucleosynthesis is calculated by interpolating the results of Gallino et al. (1998), using a grid of inter-shell abundances for different values of stellar mass, metallicity,  $^{13}\text{C}_{\text{eff}}$  and thermal pulse number. We investigate a fine grid of initial stellar masses and we follow the time evolution of the surface abundances in each star. We explore the ratio of the heavy *s*-process element (hs) average abundance to the light *s*-process element (ls) average abundance

$$\left[ \frac{\text{hs}}{\text{ls}} \right] = \left( \left[ \frac{\text{Ba}}{\text{Fe}} \right] + \left[ \frac{\text{La}}{\text{Fe}} \right] + \left[ \frac{\text{Ce}}{\text{Fe}} \right] + \left[ \frac{\text{Nd}}{\text{Fe}} \right] + \left[ \frac{\text{Sm}}{\text{Fe}} \right] \right) * 0.2 - \left( \left[ \frac{\text{Y}}{\text{Fe}} \right] + \left[ \frac{\text{Zr}}{\text{Fe}} \right] \right) * 0.5$$

in 100 TP-AGB stars for each metallicity in a range of initial masses from  $1.0$  to  $8.0 M_{\odot}$ . We have taken into account 25 different metallicities in the range  $-2.3 < [\text{Fe}/\text{H}] < 0.1$  and for each one we have weighted the output of the different masses by the IMF of Kroupa, Tout & Gilmore (1993).

The population synthesis is carried out for different values of  $^{13}\text{C}_{\text{eff}}$  and the output is compared to observational data, as described below.

## 3. Comparison of results with observations

### 3.1. Intrinsic *S*-enhanced stars

In the context of single stellar evolution it is straightforward to compare the output of the population synthesis with the observed intrinsic *s*-enhanced stars. The first set of data that we compare to are the intrinsic MS/S stars of Busso et al. (2001), for which we select from the synthesized population the stars that have a surface effective temperature less than  $3500 \text{ K}$  and that are not carbon stars, i.e.,  $\text{C}/\text{O} < 0.95$ . As can be seen in Fig. 1a, the observations can be fitted quite well with just one  $^{13}\text{C}$  efficiency value,  $^{13}\text{C}_{\text{eff}} = 2$ .

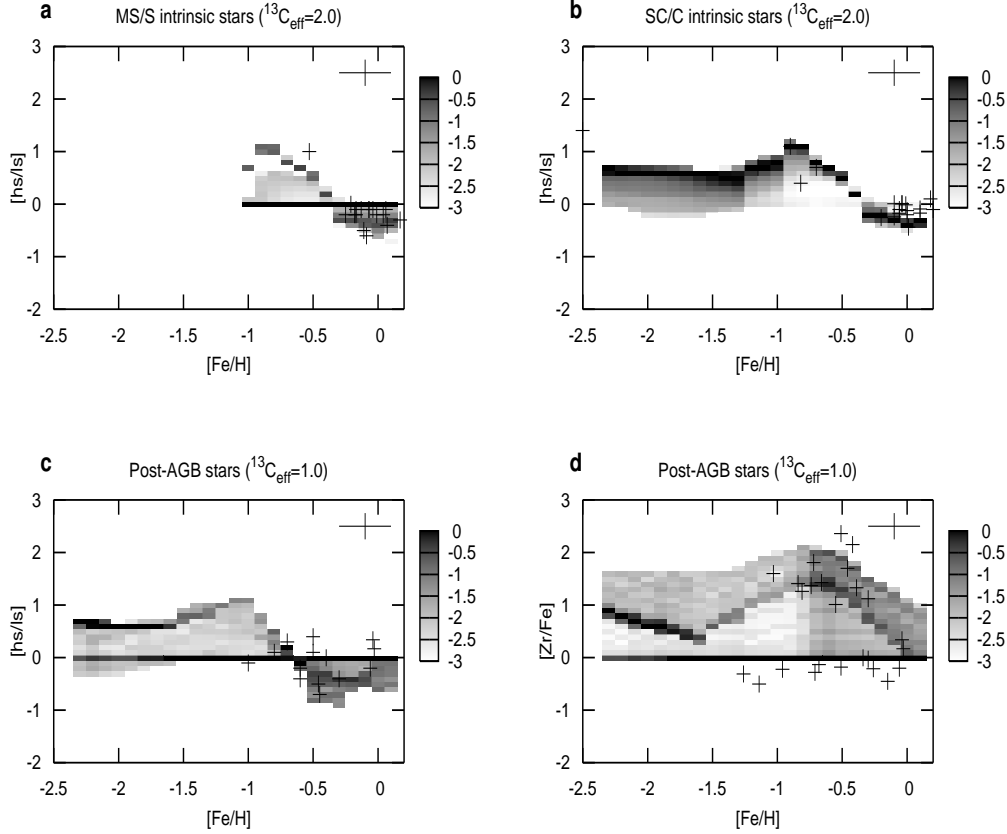


**Fig. 1.** Intrinsic *s*-enhanced stellar population synthesis results compared against the observations. The gray scale is a logarithmic measure of the number distribution of stars over  $[\text{hs}/\text{ls}]$  or (in panel d)  $[\text{Zr}/\text{Fe}]$ . The crosses are the observational data (see the references in the text), which have an average error given by the size of the upper right cross in each plot. The number density is weighted by the IMF and by the time each star spends in an abundance bin, and then normalized for each metallicity.

The next set are intrinsic SC and C stars, taken from Busso et al. (2001) and from Abia et al. (2002). Our synthesized SC and C stars are those TP-AGB stars which have  $\text{C}/\text{O} > 0.95$ . Again, from Fig. 1b it can be seen that with only  $^{13}\text{C}_{\text{eff}} = 2$  the data is well fitted, without the need for a spread in  $^{13}\text{C}_{\text{eff}}$ .

The last set of intrinsic stars to compare to are the post-AGB stars, taken from Busso et al. (2001), Van Winckel (2003),

Giridhar & Arellano (2005) and Gallino et al. (2005). We have considered as post-AGB stars all those from our synthetic TP-AGB sample which have an envelope mass of  $0.02 M_{\odot}$  or less. Most of them can be well fitted with  $^{13}\text{C}_{\text{eff}} \approx 1$  (Fig. 1c), with a few exceptions which need  $^{13}\text{C}_{\text{eff}} \sim 1.5$ . It is important also to notice that there is an apparent split in the observed  $[\text{Zr}/\text{Fe}]$ , which suggests that some post-AGB stars (those with  $[\text{Zr}/\text{Fe}] \approx 0$ ) did not

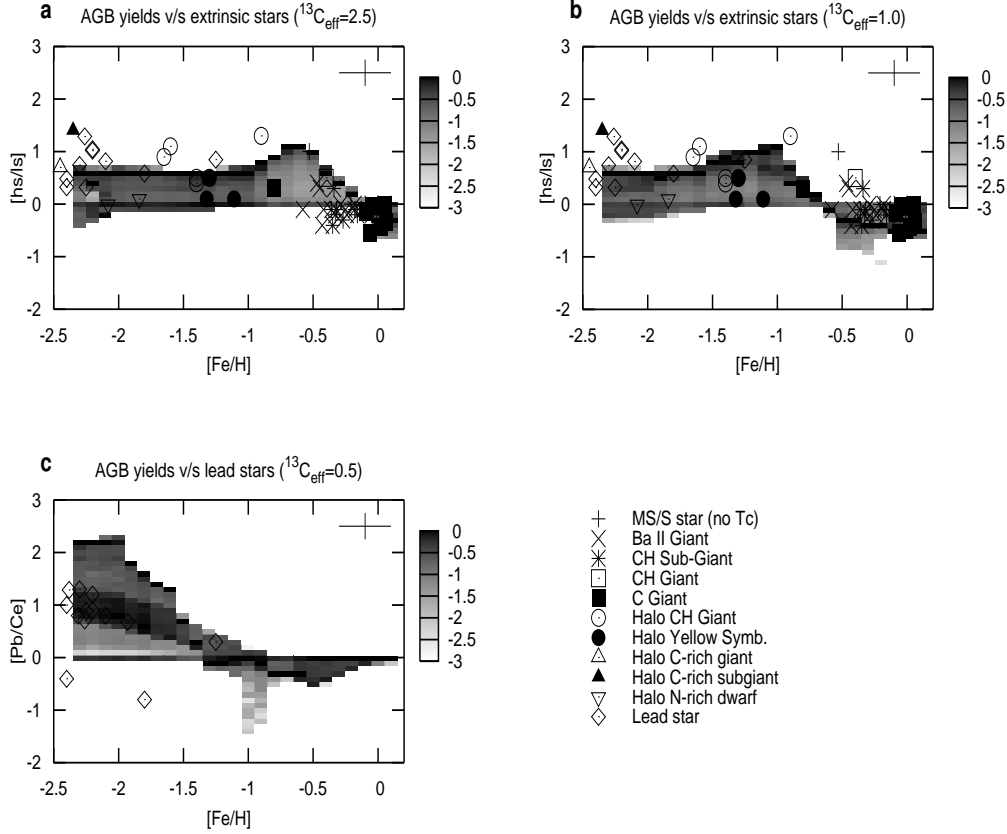


**Fig. 2.** Population synthesis yield results compared against observations of extrinsic  $s$ -enhanced stars. The gray scale is a logarithmic distribution of the yield ratios ( $[\text{hs}/\text{ls}]$  and  $[\text{Pb}/\text{Ce}]$ ) for a population of stars as a function of metallicity. The points are observed data from different references (see text), which have an average error given by the size of the upper right cross in each plot. The results are weighted by the IMF and normalized for each metallicity.

experience dredge-up episodes, while others (those highly  $s$ -process enhanced) did experience dredge-up (Van Winckel, 2003). This dichotomy is also observed in our results and is consistent with  $^{13}\text{C}_{\text{eff}} \approx 1$  for these stars, as can be seen in Fig. 1d.

### 3.2. Extrinsic $S$ -enhanced stars

Extrinsic  $s$ -enhanced stars can also be studied with single stellar population synthesis

albeit only in an approximate way. As these stars are formed by accreting mass from an  $s$ -enhanced companion, their abundance enhancements are (to first order) proportional to the mass of the various elements yielded by their companions. We thus compare to the yields, rather than to the surface abundances, of our synthesized TP-AGB stars, again weighted by the IMF. Comparing the population synthesis yields with the extrinsic star data of Busso

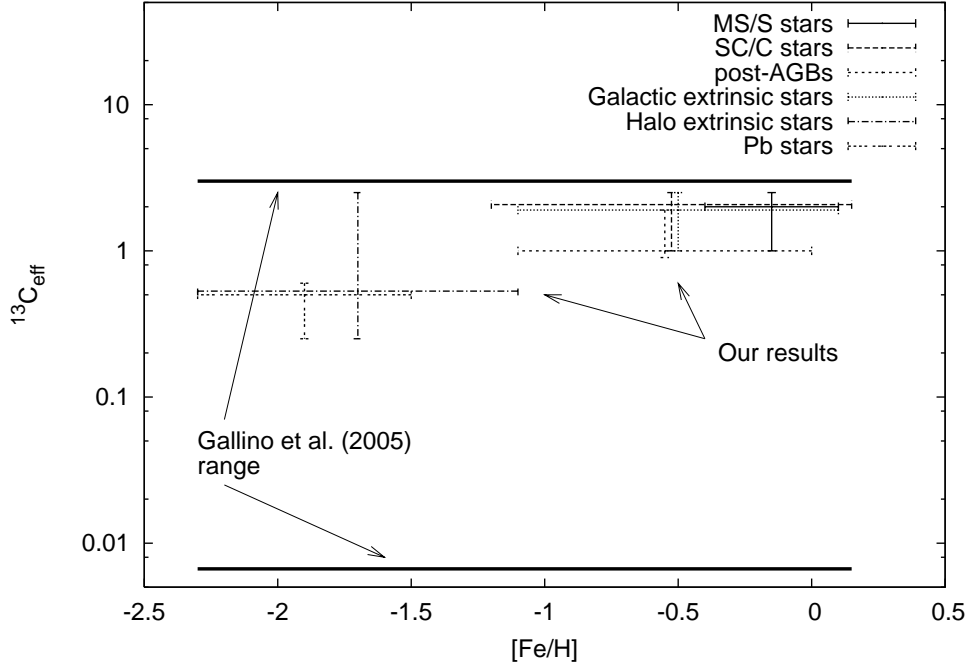


**Fig. 3.** Range of  $^{13}\text{C}_{\text{eff}}$  for which the observations of different kinds of *s*-enhanced stars are reproduced by population synthesis and the metallicity range within which they are observed. The thick solid lines show the range of  $^{13}\text{C}_{\text{eff}}$  needed by Gallino et al. (2005) to reproduce the observations.

et al. (2001) and Abia et al. (2002) we see in Figs. 2a and 2b that the  $[\text{hs}/\text{ls}]$  ratios of these stars are well reproduced with  $1 \lesssim ^{13}\text{C}_{\text{eff}} \lesssim 3$ , which is consistent with the values found for the intrinsic *s*-enhanced stars.

At  $[\text{Fe}/\text{H}] \lesssim -1$  there are no intrinsic stars nor is the  $[\text{hs}/\text{ls}]$  ratio very sensitive to  $^{13}\text{C}_{\text{eff}}$  changes. It is at this point that the role of lead stars becomes important. They are low metallicity *s*-enhanced extrinsic stars on which Pb has been detected. The  $[\text{Pb}/\text{hs}]$  ratios are sensitive to the value of  $^{13}\text{C}_{\text{eff}}$ . In particular we compute the  $[\text{Pb}/\text{Ce}]$  ratios and compare our models to the data of Van Eck et al. (2003) and references therein. We find that for most of the lead star  $[\text{Pb}/\text{Ce}]$  ratios can be reproduced with  $^{13}\text{C}_{\text{eff}} \approx 0.5$  (see Fig. 2c), except for two clear outliers.

#### 4. Conclusions

We have found that in order to reproduce the different  $[\text{hs}/\text{ls}]$  and  $[\text{Pb}/\text{Ce}]$  ratios observed in *s*-enhanced stars only a small spread in the  $^{13}\text{C}$  efficiency is needed. The observed spread in element ratios can be naturally explained by different initial stellar masses and the time evolution of the TP-AGB stars, and it is not necessary to use the large spread of  $^{13}\text{C}_{\text{eff}}$  values (more than two orders of magnitude) suggested by other works, e.g., Busso et al., 2001, Gallino et al., 2005, and references therein. Galactic disk objects ( $[\text{Fe}/\text{H}] \gtrsim -1$ ) are well reproduced by considering the range  $1 \lesssim ^{13}\text{C}_{\text{eff}} \lesssim 3$  in our population synthesis. Most halo objects (low-metallicity stars) are well reproduced with  $^{13}\text{C}_{\text{eff}} \approx 0.5$ . This might suggest that at low metallicities  $^{13}\text{C}_{\text{eff}}$  is smaller. Fig. 3 shows a sum-

mary of the range of  $^{13}\text{C}_{\text{eff}}$  values needed to reproduce the different types of stellar population, which is limited within a factor of 5.

In the results presented we did not take into account the existence of an age-metallicity relation, which limits the range of stellar masses that actually contributes to the observed intrinsic *s*-enhanced stars at each metallicity. In future work we will take this into account, and also perform a proper binary evolution population synthesis to get a more reliable outcome for the extrinsic *s*-enhanced stars.

## References

- Gallino, R.; Arlandini, C.; Busso, M.; Lugaro, M.; Travaglio, C.; Straniero, O.; Chieffi, A.; Limongi, M. 1998 ApJ, 497, 388G
- Busso, M.; Gallino, R.; Lambert, D.L.; Travaglio, C.; Smith, V.V. 2001 ApJ, 557, 802B
- Gallino, R.; Arnone, E.; Pignatari, M.; Straniero, O. 2005 Mem. S.A.It., 75, 700
- Izzard, R.G.; Tout, C.A.; Karakas, A.I.; Pols, O.R. 2004 MNRAS, 350, 407I
- Kroupa, P.; Tout, C.A.; Gilmore, G. 1993 MNRAS, 262, 545K
- Abia, C.; Domnguez, I.; Gallino, R.; Busso, M.; Masera, S.; Straniero, O.; de Laverny, P.; Plez, B.; Isern, J. 2002 ApJ, 579, 817A
- Van Winckel, H. 2003 ARA&A, 41, 391V
- Giridhar, S.; Arellano Ferro, A. 2005 A&A, 443, 297G
- Van Eck, S.; Goriely, S.; Jorissen, A.; Plez, B. 2003 A&A, 404, 291V
- Aoki, W.; Ryan, S.G.; Norris, J.E.; Beers, T.C.; Ando, H.; Tsangarides, S. 2002 ApJ, 580, 1149A